POLITECNICO DI TORINO
Repository ISTITUZIONALE

Accelerated assessment of optimal fuel economy benchmarks for developing the next generation HEVs

Original
Accelerated assessment of optimal fuel economy benchmarks for developing the next generation HEVs / Anselma, PIER GIUSEPPE; Belingardi, Giovanni. - 20. Internationales Stuttgarter Symposium:(2020), pp. 623-639. (20th Stuttgart International Symposium - Automotive and Engine Technology Stuttgart (Germany) 17-18 March 2020) [10.1007/978-3-658-30995-4_52].

Availability:
This version is available at: 11583/2837680 since: 2020-09-30T11:12:31Z

Publisher:
Springer

Published
DOI:10.1007/978-3-658-30995-4_52

Terms of use:

This article is made available under terms and conditions as specified in the corresponding bibliographic description in the repository

Publisher copyright
Springer postprint/Author's Accepted Manuscript

This version of the article has been accepted for publication, after peer review (when applicable) and is subject to Springer Nature's AM terms of use, but is not the Version of Record and does not reflect post-acceptance improvements, or any corrections. The Version of Record is available online at: http://dx.doi.org/10.1007/978-3-658-30995-4_52

(Article begins on next page)

07 May 2026

Accelerated assessment of optimal fuel economy benchmarks for developing the next generation HEVs

Pier Giuseppe Anselma, Giovanni Belingardi

Department of Mechanical and Aerospace Engineering (DIMEAS)
Center for Automotive Research and Sustainable Mobility (CARS)
Politecnico di Torino, Torino, Italy

1 Introduction

Hybrid electric vehicles (HEVs) are forecasted remarkably spreading in the global vehicle market over the next years due to their capability of reducing fuel consumption and tailpipe emissions while simultaneously tackling current limitations for on-board storable electrical energy [1]. Nevertheless, design procedures and sizing methodologies for HEV powertrains are consistently complicated compared to both battery electric vehicles (BEVs)that are powered by electric motors solely, and conventional vehicles that are powered by internal combustion engines (ICEs) solely [2]. Difficulties in HEV powertrain design and sizing relate both to the amount of power components embedded (i.e. one ICE, one or multiple electric motor/generators (MGs), a high-voltage battery, dedicated power electronics) and the necessity of a related proper energy management strategy (EMS) [3].

EMSs for HEVs can be classified into off-line and on-line ones. Off-line EMSs profit from the overall knowledge of preselected driving missions to optimize the HEV powertrain operation. They can be used to assess the fuel economy capability of HEV powertrain architectures and component sizes [4][5] or to calibrate and benchmark on-line EMSs [6][7][8]. On the other hand, on-line EMSs do not require the knowledge of future driving conditions and they can therefore be implemented in the on-board ECU of HEVs. This paper focuses on off-line EMSs for HEVs. In this framework, examples of popular optimization strategies for HEVs include Dynamic Programming (DP), the Pontryagin's Minimum Principle (PMP) and the Power-weighted Efficiency-based Analysis for Rapid Sizing (PEARS) [9]. DP represents the most popular HEV optimization approach as it can return a global optimal solution, nevertheless it suffers from curse of dimensionality [10]. The PMP can approximate the global optimal solution provided by DP under few assumptions, however it does not always guarantee the global optimum and requires the calibration of the tuning factor for the electrical energy consumption [11]. The PEARS algorithm is computationally rapid and it can satisfy the charge-sustaining criterion without recurring to iterative calculation, however it exhibits non-uniform proximity with the global optimum and it can be applied to a limited set of HEV architectures represented by the multimode power split powertrains [12]. Therefore, there remains a need for a validated universal off-line control strategy suitable for rapid sizing of all types of HEV powertrains [13].

To answer the illustrated drawbacks, this paper aims at presenting a new off-line EMS for HEVs suitable for rapid sizing of hybrid powertrain components named Slope-weighted Energy-based Rapid Control Analysis (SERCA). This EMS has been developed aiming at achieving a good approximation of the optimal HEV fuel economy benchmark provided by DP while simultaneously reducing the computational cost by

around two orders of magnitude. Moreover, the SERCA algorithm can be easily implemented for different kind of HEV powertrain architectures including parallel, series-parallel and power split. The rest of this paper is organized as follows: the HEV powertrain architectures under study are firstly presented and modeled. The off-line optimal control problem is then introduced for all the retained HEV architectures. DP is subsequently recalled as global optimal, yet computationally expensive, benchmark EMS. SERCA is then illustrated and implemented for all the HEV layouts. Simulation results and conclusions are finally given.

2 HEV powertrain architectures and modeling

This section firstly aims at presenting the considered HEV powertrain architectures including parallel, series-parallel and power split layouts. Then, the adopted HEV modeling approach will be discussed.

2.1 HEV powertrain layouts

2.1.1 Parallel P2

Among the different hybrid architectures, parallel HEVs have been selected by many car manufacturers as their first step into vehicle electrification [14]. In a parallel HEV, the tractive power is combined: both the ICE and the MGs can contribute to the vehicle propulsion, i.e. their corresponding torques are additive. When the MG is large enough, it can drive the HEV by itself or simultaneously with the ICE. Particularly, the MG can be used to shift the ICE operating points to a higher-efficiency area by acting as a generator or a motor depending on the power demand being higher or lower. Particularly in the P2 architecture, one MG is placed between the ICE and the gearbox input and a clutch connection allows for eventually disengaging it from the ICE crankshaft. A possible scheme of the parallel P2 HEV layout is illustrated in Figure 1.

2.1.2 Series-Parallel P1P2

Series-parallel HEV powertrain architectures embed two MGs. Particularly for the P1P2 layout, other than the MG located in the P2 position, an additional MG is mounted directly on the ICE crankshaft as shown in Figure 2. When the clutch is engaged, ICE, MG1 and MG2 exhibits the same angular speed and the propelling torque can be arbitrarily distributed among these three power components. On the other hand, when the clutch is disengaged, the HEV powertrain can either operate in pure electric mode (i.e. ICE and MG1 are not activated) or in series mode (i.e. the ICE is turned on and MG1 serves as generator in providing electrical energy to the battery).

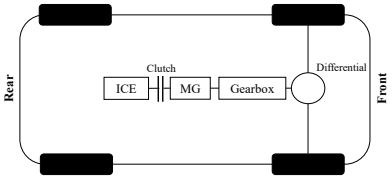

Figure 1: Parallel P2 HEV layout

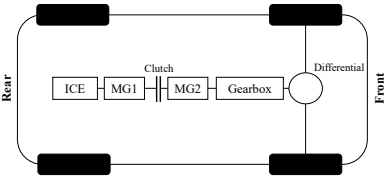

Figure 2: Series-Parallel P1P2 HEV layout

2.1.3 Power split

Power split HEV architectures are much successful and represent a large portion of the current population of commercially available full HEV powertrains. They consist of one or multiple planetary gear (PG) sets, which are very compact and can realize a continuously variable transmission. PG sets embed a ring gear, a sun gear and a carrier and they constitute the power split device (PSD), which is responsible for directing the power fluxes between the components of the hybrid powertrain [15]. Thanks to the PG kinematics, in a power split HEV the rotating speed of the ICE can be decoupled from the speed of the vehicle, thus enhancing fuel economy potential and flexibility in the operation. The power split HEV layout retained in this paper is illustrated in Figure 3 and refers to the well-known Toyota Hybrid System® [16]. In this HEV configuration, ICE, MG1 and output shaft are respectively linked to carrier, sun gear and ring gear of a PG set, while MG2 is directly linked to the output shaft through a reduction gearset.

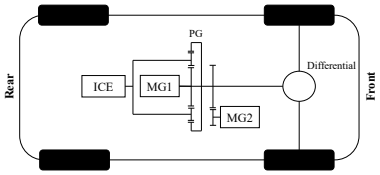

Figure 3: Power split HEV layout

2.2 HEV powertrain modeling

Overall, the HEV powertrain architectures considered in this paper are modelled adopting a backward quasi-static approach [17]. In this modeling procedure, required speed, torque and power values for the hybrid powertrain components are directly derived from the vehicle speed profile defined in the retained driving mission. In other words, the actual vehicle speed always matches the targeted profile of the driving mission. The power components (i.e. ICE and MGs) are taken into account through their empirical

operational maps with torque and speed as independent variables, while an internal resistance model is adopted for the battery. Here, values for voltage and internal resistance are assumed to be constant and independent from the battery state-of-charge (SoC), as it has been demonstrated that it is still possible to achieve a globally optimal solution with this hypothesis for charge-sustaining (CS) problems [18].With regards to the vehicle, road resistance forces are evaluated using experimental road load coefficients. More details about the powertrain and vehicle model can be found in [4].

3 Off-line HEV control

In this section, the HEV off-line control problem is presented that is typically considered in HEV powertrain design and sizing processes and in development and calibration procedures of on-line EMSs. Subsequently, DP is recalled as universally accepted numerical tool to return the global optimal solution for the HEV off-line control problem.

3.1 Control problem

The optimal off-line control problem for an HEV aims here at minimizing a multi-target cost function J that considers, among other terms, estimated fuel consumption (EFC) and number of ICE activations over a certain period as example. The resulting mathematical formulation is stated in (1):

$$\min\left\{ J = \int_{t_0}^{t_{end}} L_{P_i}(t)dt \right\}$$

subject to:

$$\begin{aligned}
SoC(t_0) &= SoC(t_{end}) \\
\dot{SOC} &= f(SOC, \omega_{MG1}, T_{MG1}, \omega_{MG2}, T_{MG2}) \\
\omega_{ICE_{min}} &\le \omega_{ICE} \le \omega_{ICE_{MAX}} \\
\omega_{MG1_{min}} &\le \omega_{MG1} \le \omega_{MG1_{MAX}} \\
\omega_{MG2_{min}} &\le \omega_{MG2} \le \omega_{MG2_{MAX}} \\
T_{ICE_{min}} &\le T_{ICE} \le T_{ICE_{MAX}} \\
T_{MG1_{min}} &\le T_{MG1} \le T_{MG1_{MAX}} \\
T_{MG2_{min}} &\le T_{MG2} \le T_{MG2_{MAX}} \\
P_{batt_{min}} &\le P_{batt} \le P_{batt_{MAX}} \\
SoC_{min} &\le SoC \le SoC_{MAX}
\end{aligned} \tag{1}$$

Where $L_{P_i}(t)$ represents the instantaneous cost function which needs specific definition depending on the retained HEV powertrain architecture P_i as it will be detailed later in this section. Charge-sustaining (CS) criteria is defined by imposing equivalent battery SoC values at the beginning and the end of the considered time period. Finally, speed, torque and power of power components (battery, ICE, MG1 and MG2 as well where applicable) are restricted within the correspondent actual operating regions. In the follow-up of this section, DP will be illustrated as numerical approach to solve this control problem.

3.2 Dynamic Programming

DP is by far the most commonly adopted approach to solve the HEV optimal control problem. It involves generating a globally optimal solution backward along a time horizon by searching through all feasible discrete control actions for all the state grid points [19]. While DP is demonstrated achieving global optimality under a wide range of operating conditions, its major drawback refers to the computational power and computational time needed for exhaustively searching through all the possible solutions [20]. Specifically considered control variables, state variables and cost functions for the retained HEV powertrain layouts will be illustrated below.

3.2.1 Parallel P2

When controlling a parallel P2 HEV, three levels of decision need accomplishment at each time instant [7]:

1 Which gear is to be engaged in the gearbox;

2 Whether to propel the vehicle in pure electric mode (MG only) or in hybrid operation (ICE+MG);

3 In case the hybrid mode is selected, how to split the required torque between ICE and MG.

This leads to embed the two terms illustrated in (2) for the control variable U_{P2} including the gear number $\#_{gear}$ and the value of ICE torque T_{ICE}.

$$U_{P2} = \begin{Bmatrix} \#_{gear} \\ T_{ICE} \end{Bmatrix} \tag{2}$$

In a backward HEV modelling approach, pure electric or hybrid operation are particularly distinguished by the sign of the ICE torque being null or positive, respectively. As regards the state variable X_{P2}, its formulation considered here is reported in (3).

$$X_{P2} = \begin{Bmatrix} SoC \\ ICE_{on/off} \\ \#_{gear} \end{Bmatrix} \quad (3)$$

The battery SoC is retained in order to achieve CS operation, while a binary term defining the ICE state (i.e. on/off) and the engaged gear number are considered in order to account for comfort and smooth HEV operation. Particularly, the optimal control solution identified by DP throughout the driving mission should avoid an excessive number of ICE de/activation and gear shifting events. This is performed by formulating the instantaneous cost function (whose integrated value over the driving mission needs minimization) L_{P2} as follows:

$$L_{P2} = \dot{m}_{fuel} + \alpha_1 \cdot ICE_{start} + \alpha_2 \cdot gear_{shift} \quad (4)$$

Where $\dot{m}_{fuel}$ represents the instantaneous rate of fuel consumption as given by the ICE fuel table, while ICE_{start} and $gear_{shift}$ denote ICE activation and gear shifting events, respectively, which can be detected by means of the corresponding state terms. α_1 and α_2 are constant weighting factors.

3.2.2 Series-Parallel P1P2

The required control decisions for a series-parallel P1P2 layout are similar to the ones related to the parallel P2 HEV architecture, yet few additions need to be made. Obtained levels of decisions are reported as follows:

1 Which gear is to be engaged in the gearbox;

2 Whether to keep the clutch engaged or disengaged;

3 In case the clutch is engaged, how to split the required torque between ICE, MG1 and MG2;

4 In case the clutch is disengaged, whether to operate in pure electric mode (i.e. only MG2 is activated) or in series mode (ICE and MG1 are activated as well);

5 In case the series hybrid operation is selected, which values of speed and torque assign to ICE and MG1.

As a result, the corresponding control variable U_{P1P2} requires additional terms to handle the increased control complexity for this HEV layout, namely the MG1 torque T_{MG1}, the ICE speed ω_{ICE} and the binary clutch status $Cl_{eng/dis}$ (i.e. engaged or disengaged):

$$U_{P1P2} = \begin{Bmatrix} \#_{gear} \\ T_{ICE} \\ T_{MG1} \\ \omega_{ICE} \\ Cl_{eng/dis} \end{Bmatrix} \tag{5}$$

As concerns state variable X_{P1P2} and cost function L_{P1P2}, their formulations for the series-parallel P1P2 HEV architecture equal their counterparts for the parallel P2 layout.

3.2.3 Power split

Power split HEV powertrain layouts exhibit different terms in their control variables compared to parallel and series-parallel architectures. The control variable U_{PS} considered in this paper for the power split HEV layout contains speed and torque values for the ICE and it is formulated in (6).

$$U_{PS} = \begin{Bmatrix} \omega_{ICE} \\ T_{ICE} \end{Bmatrix} \tag{6}$$

In a backward modeling approach, values of speed and torques for both the MGs can indeed be evaluated starting from the control variable terms following the planetary gear kinematics and dynamics [15]. In the considered power split HEV layout, the embedment of a gearbox is not strictly necessary in the hybrid transmission since the capability of PG sets of operating as an electrically variable transmission (eVT). As consequence, the state variable X_{PS} and the cost function L_{PS} for the power splti HEV architecture can be simplified as in (7) and (8), respectively.

$$X_{PS} = \begin{Bmatrix} SoC \\ ICE_{on/off} \end{Bmatrix} \tag{7}$$

$$L_{PS} = \dot{m}_{fuel} + \alpha_1 \cdot ICE_{start} \tag{8}$$

4 Slope-weighted Energy-based Rapid Control Analysis (SERCA)

In this section, the Slope-weighted Energy-based Rapid Control Analysis (SERCA) is described as a novel approach for the HEV off-line optimal control problem. This methodology can be divided in three phases, as illustrated in Fig. 4: the division into subproblems, the definition of the generalized optimal operating points and the energy balance realization process [21][22].

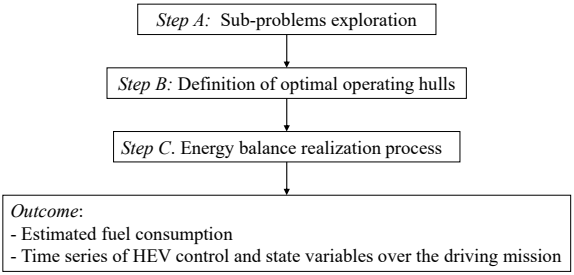

Figure 4: Workflow of SERCA

4.1 Sub-problems exploration

The first step of SERCA aims at exploring the possible solutions of each sub-problem, particularly represented by the single time point of the retained driving mission. The sub-problems are characterized with the specific values of current vehicle speed and desired acceleration, respectively. Similar to DP, discretized arrays for the control variable terms are firstly created. Each possible control sub-solution for the specific sub-problem is thus represented by a certain combination of control term values. Following the backward HEV modeling approach, values for EFC and variation in the battery SoC can then be assessed for each feasible sub-solution.

4.2 Definition of optimal operating hulls

Once all the possible sub-solutions are identified for a specific subproblem (i.e., a time point of a target driving mission), they can be assessed based on EFC and battery SoC depletion. Examples of sub-solution comparisons for the same sub-problem corresponding to a current vehicle speed value of 35 km/h and a requested vehicle acceleration from the driver of 0.1 m/s^2 are illustrated in Fig. 5, Fig. 6 and Fig. 7 for the parallel, the series-parallel and the power split HEV layouts, respectively. In all the three figures, a positive value of SoC depletion means that the battery is providing energy to power the vehicle. This corresponds both to pure electric operation and to hybrid operation in case the ICE is not providing enough power to propel the vehicle by itself. On the other hand, a negative value of battery depletion means that the ICE is providing more power than the amount needed to satisfy the power demand coming from the algebraic sum of vehicle resistance forces and inertia load related to the requested vehicle acceleration. In this case, the excess ICE power can be used to charge the high-voltage battery.

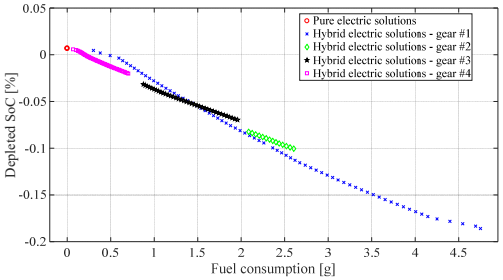

Figure 5: Sub-solutions comparison example for a parallel P2 HEV layout (vehicle speed = 35 km/h, vehicle acceleration = 0.1 m/s^2)

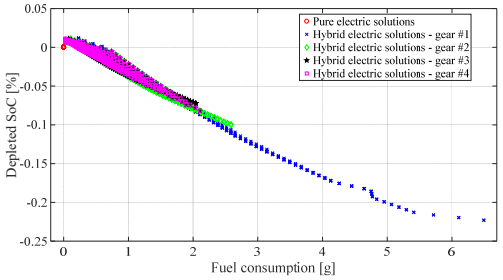

Figure 6: Sub-solutions comparison example for a series-parallel P1P2 HEV layout (vehicle speed = 35 km/h, vehicle acceleration = 0.1 m/s^2)

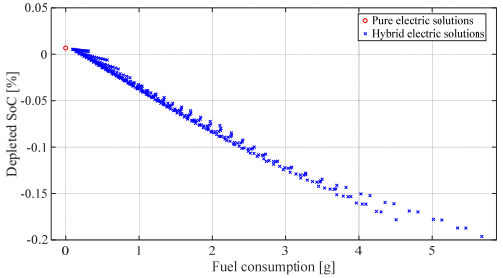

Figure 7: Sub-solutions comparison example for a power split HEV layout (vehicle speed = 35 km/h, vehicle acceleration = 0.1 m/s^2)

The general descending trend of the point cloud reminds how battery recharging can be achieved through the gradual increase of fuel consumption. The shape of the cloud of points for the hybrid electric sub-solutions differs according to the specifically retained HEV powertrain layout as shown in Fig. 5, Fig. 6 and Fig. 7, respectively. As example, for the P2 HEV layout in Fig. 5, a single curve can be observed for each feasible gear number that can be traced by varying the value set to the ICE torque. On the other hand, for series parallel P1P2 and power split architectures in Fig. 6 and Fig. 7 respectively, a cloud of points can be recognized rather than single curves. This is due to the additional degree of freedom related to the capability of varying the speed of the ICE.

This representation can be interpreted as a sort of Pareto frontier for all the feasible sub-solutions of the HEV powertrain in the considered sub-problem. The sub-solutions at the lower edge of the point cloud thus correspond to the optimal ones, as they exhibit the highest ratio between charged battery energy and correspondently consumed fuel. As consequence, these sub-solutions should be considered for eventual hybrid operation in an attempt of reaching the global optimal solution in a considered driving mission. A discrete operating hull is therefore stored for each sub-problem that is represented by the optimal sub-solutions of the Pareto frontier. Then, the slope between two adjacent points *(k-1)* and *k* of the optimal hull is defined as θ in (9).

$$\theta(k-1,k) = \frac{\Delta \dot{SoC}}{\Delta \dot{m}_{fuel}} = \frac{\dot{SoC}(k) - \dot{SoC}(k-1)}{\dot{m}_{fuel}(k) - \dot{m}_{fuel}(k-1)} \tag{9}$$

After the optimal operating hull is identified and stored and the slope for each optimal sub-solution is computed for all the sub-problems of the considered driving mission, the energy balance realization process can be performed.

4.3 Energy balance realization process

The last stage of SERCA aims at efficiently solving the optimal HEV off-line control problem for the overall considered driving mission.

First it is assumed that, when feasible, the HEV powertrain operates all the time points in pure electric mode. Particularly, in the Pareto frontiers of Fig. 5, Fig. 6 or Fig. 7 the pure electric point with the lowest depleted SoC value is considered and the hybrid powertrain is set to operate according to the corresponding control variables in the considered sub-problem. The total required electrical energy E_{EV} is then obtained by summing the depleted (or charged) battery energy in each point where pure electric mode is selected.

Consequently, the time point *i* exhibiting the highest value of slope ($|\theta_i| = |\theta_{MAX}|$) is selected for hybrid operation. The corresponding control variables are set to operate in

the identified time point. Then, the variables related to the overall driving mission operation are updated in (10).

$$\begin{aligned} \mathrm{E}_{EV} &= \mathrm{E}_{EV} + SoC_{depleted_i} \\ \mathrm{m}_{fuel\_TOT} &= \mathrm{m}_{fuel\_TOT} + \mathrm{m}_{fuel_i} \end{aligned} \tag{10}$$

Particularly, the value of required electrical energy needed is reduced by the charged battery energy in correspondence with the selected point *i*. Meanwhile, the global fuel consumption m_{fuel_TOT} is increased with the increment provided by the selected hybrid operating point.

The electric-to-hybrid operation replacement is carried out iteratively until the value of overall electrical energy consumed in the retained driving mission E_{EV} becomes null or negative. Finally, the corresponding EFC and the hybrid powertrain operation for the considered driving mission can be extrapolated in this way.

5 Simulation results

The SERCA algorithm aims at achieving optimality for the HEV off-line control problem solution and simultaneously reducing the associated computational cost. In this section, several driving missions are considered to evaluate the performance of SERCA when applied to various HEV powertrain architectures while benchmarking it with the well-known DP approach. Table 1 illustrates the vehicle and powertrain data considered in this paper. In general, vehicle and battery data for a full HEV model have been retained from Amesim® software, while lookup tables for power components and battery have been derived from [23] and scaled appropriately in order to get an hybridization factor of around 0.45 for all the three HEV considered architectures [24].

Table 1. Vehicle and powertrain data

Component	Parameter	Value
Vehicle	Mass	1000 Kg
	Wheel dynamic radius	0.317 m
	Road Load coefficient A	100 N
	Road Load coefficient B	5 N/(m/s)
	Road Load coefficient C	0.5 N/(m/s)^2
ICE	Capacity	1.2 l
	Maximum power	89 kW @ 4000 rpm
	Maximum torque	230 Nm @ 2000 rpm
Transmission (P1 and P1P2 layouts)	Gear ratios	[3.7; 2; 1.5; 1; 0.8]
	Final drive ratio	3

Transmission (power split layout)	PG ratio (ring/sun)	3.27
	MG2 to output shaft ratio	1.26
	Final drive ratio	3.27
MG (P2 layout)	Maximum power	72 kW
	Maximum torque	240 Nm
MG1 (P1P2 and power split layouts)	Maximum power	22 kW
	Maximum torque	74 Nm
MG2 (P1P2 and power split layouts)	Maximum power	50 kW
	Maximum torque	167 Nm
Battery	Capacity	19 Ah
	Open-circuit voltage	123.62 V
	Internal resistance	54.54 mΩ
	Temperature	25 °

Driving missions simulated here particularly refer to the Urban Dynamometer Driving Schedule (UDDS), the Highway Fuel Economy Test (HWFET), the Worldwide Harmonized Light Vehicles Test Procedure (WLTP) and the New European Driving Cycle (NEDC). All the reported computational times (CTs) refer to a desktop computer with Intel Core i7-8700 (3.2 GHz) and 32 GB of RAM. In all the simulations, a CS operation has been simulated by imposing equal battery SoC values at the beginning and the end of the driving missions.

Table 2 and Table 3 report obtained simulation results for all the retained HEV powertrain architectures focusing on the EFC and the CT, respectively. Concerning EFC, the SERCA algorithm is demonstrated capable of predicting fuel economy results close to the DP global optimal benchmark over different driving missions. Considering the UDDS as example, the increase in the EFC value obtained by SERCA is limited within 0.76 %, 0.13 % and 0.85 % for the P2, P1P2 and power split hybrid powertrain architectures, respectively. On the other hand, looking at CTs, the SERCA algorithm is proven achieving remarkable savings compared to the DP benchmark. In the UDDS case as example, CTs required to perform a simulation using SERCA only represent the 1.46 %, 0.09 % and the 14.05 % of the DP counterpart for the P2, P1P2 and power split hybrid powertrain layouts, respectively, while giving comparable values for the EFC. In this framework, the SERCA reveals more efficient compared to the current state-of-art. The objective realization of the CS HEV operation particularly allows avoiding recursive calculation, thus suggesting the successful implementation of SERCA for effective rapid sizing of hybrid powertrain architectures.

Table 2. Simulation results for EFC

	P2		P1P2		Power split	
Driving mission	DP	SERCA	DP	SERCA	DP	SERCA
UDDS	293.25 g	295.49 g	234.99 g	235.29 g	243.22 g	245.28 g
HWFET	581.43 g	587.21 g	546.95 g	551.58 g	554.62 g	557.17 g
WLTP	723.47 g	723.95 g	757.74 g	766.68 g	771.54 g	779.26 g
NEDC	308.66 g	307.69 g	287.55 g	287.55 g	290.12 g	291.62 g

Table 3. Simulation results for CT

	P2		P1P2		Power split	
Driving mission	DP	SERCA	DP	SERCA	DP	SERCA
UDDS	274 s	4 s	22260 s	20 s	747 s	105 s
HWFET	115 s	2 s	13179 s	17 s	450 s	69 s
WLTP	184 s	7 s	30506 s	29 s	4584 s	289 s
NEDC	188 s	3 s	24100 s	14 s	3123 s	199 s

6 Conclusions

This paper presents the application of a novel rapid near-optimal EMS named slope-weighted energy-based rapid control analysis (SERCA) to various HEV powertrains including parallel, series-parallel and power split layouts. The operating steps of SERCA have been detailed, particularly the division into sub-problems, the construction of the generalized optimal operating hulls and the energy balance realization process. The SERCA addresses the problem of effective rapid component sizing for HEV powertrains. The illustrated energy management strategy is validated based on a comparison of the resulting SERCA EFC values with the globally optimal solution provided by DP over several driving missions. Results for several different driving missions particularly reveal a narrow difference contained within 0.99 %, 1.18 % and 1.00 % at maximum for the parallel P2, the series parallel P1P2 and the power split HEV powertrain architecture, respectively. Moreover, the SERCA algorithm is demonstrated achieving remarkable computational rapidness compared to DP.

Future work may consider the implementation of the SERCA in a design methodology for rapid component sizing of various HEV powertrains. Finally, an on-line energy management strategy may be developed based on the SERCA and implemented in an on-board control logic. For instance, offline SERCA optimization may be considered

to derive optimal control policies [25]. Alternatively, SERCA may rapidly provide near-optimal benchmarks for recently developed artificial intelligence-based on-line HEV EMSs [26].

Bibliography

1. B. Bilgin et al., "Making the Case for Electrified Transportation," in *IEEE Transactions on Transportation Electrification*, vol. 1, no. 1, pp. 4-17, 2015.

2. P.G. Anselma, G. Belingardi, “Comparing battery electric vehicle powertrains through rapid component sizing”, *Int. J. Electric and Hybrid Vehicles*, vol.11, no.1, pp. 36-58, 2019.

3. A. Biswas, A. Emadi, "Energy Management Systems for Electrified Powertrains: State-of-the-Art Review and Future Trends," in *IEEE Transactions on Vehicular Technology*, vol. 68, no. 7, pp. 6453-6467, July 2019.

4. P.G. Anselma, Y. Huo, J. Roeleveld, A. Emadi, G. Belingardi, “Rapid Optimal Design of a Multimode Power Split Hybrid Electric Vehicle Transmission”, *Proceedings of the Institution of Mechanical Engineers, Part D: Journal of Automobile Engineering*, vol. 233, no. 3, pp. 740-762, 2019.

5. P.G. Anselma, G. Belingardi, A. Falai, C. Maino, F. Miretti, D. Misul, E. Spessa, “Comparing Parallel Hybrid Electric Vehicle Powertrains for Real-world Driving”, *2019 AEIT International Conference of Electrical and Electronic Technologies for Automotive*, Torino, Italy, 2019, pp. 1-6.

6. P.G. Anselma, Y. Huo, J. Roeleveld, G. Belingardi, A. Emadi, “Real-time rule-based near-optimal control strategy for a single-motor multimode hybrid electric vehicle powertrain,” *2018 FISITA world congress*, Chennai, India, Oct. 2018, pp. 1-14.

7. P. G. Anselma, A. Biswas, J. Roeleveld, G. Belingardi and A. Emadi, "Multi-Fidelity Near-Optimal on-Line Control of a Parallel Hybrid Electric Vehicle Powertrain," *2019 IEEE Transportation Electrification Conference and Expo (ITEC)*, Detroit, MI, USA, 2019, pp. 1-6.

8. P.G. Anselma, Y. Huo, J. Roeleveld, G. Belingardi, A. Emadi, “From Off-Line to On-Line Control of a Multimode Power Split Hybrid Electric Vehicle Powertrain”, *IFAC-PapersOnLine*, vol. 52, no. 5, pp. 141-146., 2019.

9. G. Belingardi, P.G. Anselma, M. Demic, “Optimization-based controllers for hybrid electric vehicles”, in *Mobility & Vehicle Mechanics*, vol. 44, no. 3, pp. 53-67, 2018.

10. J. Lempert, B. Vadala, K. Arshad-Aliy, J. Roeleveld and A. Emadi, "Practical Considerations for the Implementation of Dynamic Programming for HEV Powertrains," *2018 IEEE Transportation Electrification Conference and Expo (ITEC)*, Long Beach, CA, 2018, pp. 755-760.

11. Kim, N., Rousseau, A.: "Sufficient conditions of optimal control based on Pontryagin's minimum principle for use in hybrid electric vehicles", *Proceedings of the Institution of Mechanical Engineers, Part D: Journal of Automobile Engineering*, Vol 226, Issue 9, 2012, pp 1160 – 1170.

12. P.G. Anselma, Y. Huo, E. Amin, J. Roeleveld, A. Emadi, G. Belingardi, "Mode-shifting Minimization in a Power Management Strategy for Rapid Component Sizing of Multimode Power Split Hybrid Vehicles," *SAE Technical Paper* 2018-01-1018, 2018.

13. P.G. Anselma, G. Belingardi, "Next generation HEV powertrain design tools: roadmap and challenges," *SAE Technical Paper* 2019-01-2602, 2019.

14. Yang, Y., Ali, K. A., Roeleveld, J., Emadi, A., "State-of-the-art electrified powertrains - hybrid, plug-in, and electric vehicles", in *International Journal of Powertrains*, vol. 5, no.1, pp.1-29, 2016.

15. Schulz M., "Circulating mechanical power in a power split hybrid electric vehicle transmission", *Proc IMeche, Part D: J Automobile Engineering*, 2004; 218: 1419–1425.

16. Matsumura, M., Shiozaki, K., and Mori, N., "Development of New Hybrid Transaxle for Mid - Size Vehicle," SAE Technical Paper 2018-01-0429, 2018.

17. L. Guzzella, A. Amstutz, "CAE tools for quasi-static modeling and optimization of hybrid powertrains", IEEE Transactions on Vehicular Technology 1999; 48(6): 1762-69.

18. N. Kim, S. Cha, and H. Peng, "Optimal Control of Hybrid Electric Vehicles Based on Pontryagin's Minimum Principle," *IEEE Transactions on Control Systems Technology*, vol. 19, no. 5, pp. 1279-1287, Sept. 2011.

19. O. Sundstrom and L. Guzzella, "A generic dynamic programming Matlab function," *2009 IEEE Control Applications, (CCA) & Intelligent Control, (ISIC)*, St. Petersburg, 2009, pp. 1625-1630.

20. J. Lempert, B. Vadala, K. Arshad-Aliy, J. Roeleveld and A. Emadi, "Practical Considerations for the Implementation of Dynamic Programming for HEV Powertrains," *2018 IEEE Transportation Electrification Conference and Expo (ITEC)*, Long Beach, CA, 2018, pp. 755-760.

21. P. G. Anselma, Y. Huo, J. Roeleveld, G. Belingardi and A. Emadi, "Slope-Weighted Energy-Based Rapid Control Analysis for Hybrid Electric Vehicles," in *IEEE Transactions on Vehicular Technology*, vol. 68, no. 5, pp. 4458-4466, May 2019.

22. G. Buccoliero, P. G. Anselma, S. Amirfarhangi Bonab, G. Belingardi and A. Emadi, "A New Energy Management Strategy for Multimode Power Split Hybrid Electric Vehicles," in *IEEE Transactions on Vehicular Technology*, in press, 2020.

23. Dabadie, J., Sciarretta, A., Font, G., and Le Berr, F., "Automatic Generation of Online Optimal Energy Management Strategies for Hybrid Powertrain Simulation," *SAE Technical Paper* 2017-24-0173, 2017.

24. J. M. Tyrus, R. M. Long, M. Kramskaya, Y. Fertman and A. Emadi, "Hybrid electric sport utility vehicles", *IEEE Transactions on Vehicular Technology* 2004; 53(5): 1607-22.

25. P. G. Anselma, Y. Huo, J. Roeleveld, G. Belingardi and A. Emadi, "Integration of On-Line Control in Optimal Design of Multimode Power-Split Hybrid Electric Vehicle Powertrains," in *IEEE Transactions on Vehicular Technology*, vol. 68, no. 4, pp. 3436-3445, April 2019.

26. A. Biswas, P. G. Anselma and A. Emadi, "Real-Time Optimal Energy Management of Electrified Powertrains with Reinforcement Learning," *2019 IEEE Transportation Electrification Conference and Expo (ITEC)*, Detroit, MI, USA, 2019, pp. 1-6.